Functional Characterization and ATP-Induced Dimerization of the Isolated ABC-Domain of the Haemolysin B Transporter†

Jelena Zaitseva,‡ Stefan Jenewein,‡ Alexander Wiedenmann,‡,|| Houssain Benabdelhak,§ I. Barry Holland,§ and Lutz Schmitt*,‡

Institute of Biochemistry, Biocenter N210, Goethe University Frankfurt, Marie-Curie Str. 9, 60439 Frankfurt, Germany, and Institut de Génétique et Microbiologie, Bât. 409, Université de Paris XI, 91405 Orsay, France

Received April 2, 2005; Revised Manuscript Received May 23, 2005

ABSTRACT: Nucleotide-binding domains (NBD) are highly conserved constituents of ATP-binding cassette (ABC) transporters. Members of this family couple ATP hydrolysis to the transfer of various molecules across cell membranes. The NBD of the HlyB transporter, HlyB-NBD, was characterized with respect to its uncoupled ATPase activity, oligomeric state, and stability in solution. Experimental data showed that both the nature and pH of an assay buffer influenced the level of protein activity. Comparative analysis of protein stability and ATPase activity in various buffers suggests an inverse relationship between the two. The highest ATPase activity was detected in HEPES, pH 7.0. A kinetic analysis of the ATPase activity in this buffer revealed an enzyme concentration dependence and ATP-induced protein oligomerization. Assuming that the dimer is the active form of enzyme, at least half of the purified HlyB-NBD was estimated to be a dimer at 1.2 μM under the most optimal conditions for ATP hydrolysis. This is about 2 orders of magnitude lower than reported for other canonical ABC-ATPases. The maximum reaction velocity of 0.6 μmol/mg·min at 22 °C and the apparent kinetic constant $K^{app}_{0.5}$ of 0.26 mM for ATP were determined for the dimerized HlyB-NBD. Gel filtration experiments with the wild-type protein and HlyB-NBD mutated in a key catalytic residue, H662A, provided further evidence for ATP-induced protein dimerization. ATPase activity experiments with protein mixtures composed of wild-type and the ATPase-deficient H662A mutant demonstrated that one intact NBD within a dimer is sufficient for ATP hydrolysis. This single site turnover might suggest a sequential mechanism of ATP hydrolysis in the intact HlyB transporter.

Pathogenic strains of *Escherichia coli* secrete virulence factors into the media to influence the metabolism of the host cells. The secretion process of haemolysin A (HlyA) in Gram-negative bacteria involves crossing both the inner and outer membrane in one step (*1*). To accomplish this task, three protein components, the outer membrane protein TolC and two inner membrane proteins, HlyB and HlyD, form a continuous channel through both membranes and the periplasmic space in *E. coli*. TolC represents a "channel-tunnel" over 140 Å long that spans the outer membrane and protrudes into the periplasmic space (*2*). HlyD, which has a small cytoplasmic and a large periplasmic domain connected via a single transmembrane helix, apparently serves as an accessory inner membrane protein completing the secretion-tunnel for the 107 kDa HlyA (*3*). HlyB is believed to form a substrate-specific pore in the inner membrane and to couple ATP hydrolysis to the unidirectional transport of HlyA.

HlyB belongs to the family of ATP-binding cassette (ABC)[1] transporters (*4*). Members of this family participate in a variety of cell processes, including secretion of proteins out of a cell (*5*), efflux of drugs (*6*), antigen presentation on the cell surface (*7*), and uptake of nutrients (*8*). ABC-machineries utilize the energy of ATP to drive the transport of substrates, the so-called allocrites, across the membranes. Typically, a complete ABC-transporter is represented by various combinations of four modules: two cytoplasmic nucleotide-binding cassettes or domains (NBDs) and two hydrophobic membrane-spanning components, the transmembrane domains (TMD) (*9*). All four substituents can be arranged in one single polypeptide or assembled from two to four separate protein subunits into a membrane-associated complex. In some ABC-transporters, however, domains can be fused to each other in a different manner. In the *E. coli* ribose transporter, two fused NBDs form the energizing part of the complex (*10*); in *Lactococcus lactis* LmrA and in human TAP, a single polypeptide contains one TMD and one NBD (*7*, *11*). On the basis of its structural organization, HlyB also belongs to the group of "half-size" ABC-transporters. According to this model, association of two HlyB molecules in the inner membrane is necessary to form

† This work was supported by CNRS at University of Paris-Sud (I.B.H.) and the Deutsche Forschungsgemeinschaft (Grant Schm1279/2-3 and SFB 628 to L.S.).

* Address for correspondence: Lutz Schmitt, Institute of Biochemistry, Biocenter N210, Johann-Wolfgang Goethe University Frankfurt, Marie-Curie Str. 9, 60439 Frankfurt, Germany. Tel, +49(0)69-79829-569; fax, +49(0)69-79829-495; e-mail, lschmitt@em.uni-frankfurt.de.

‡ Goethe University Frankfurt.

§ Université de Paris XI.

|| Present address: Institute of Microbiology, ETH Zürich, Schmelzbergstr. 7, 8092 Zürich, Switzerland.

[1] Abbreviations: ABC, ATP-binding cassette; Hly, haemolysin; NBD, nucleotide-binding domain; SAC, substrate-assisted catalysis; SEC, size exclusion chromatography; TMD, transmembrane domain; wt, wild-type.

10.1021/bi0506122 CCC: $30.25
Published on Web 06/23/2005

a functional ABC complex. Each HlyB protein has an N-terminal hydrophilic portion (amino acid residues 1−150), followed by a hydrophobic membrane domain and a conserved 28 kDa cytoplasmic NBD (*1*).

NBDs of different ABC-transporters share significant sequence identity. Recent studies of various isolated NBDs have also revealed their overall structural conservation despite the huge diversity of allocrites (*12*). This allows one to postulate a common mechanism of ATP-binding/hydrolysis for ABC-transporters with different functions. Nevertheless, although TMDs generally determine allocrite specificity, small but important differences in structure and biochemical properties of different NBDs exist, which are probably linked to allocrite recognition (*13, 14*). Although many intensive studies of whole ABC-complexes and their isolated NBD components have been completed (*1, 15, 16*), we are still far from understanding their mechanism of action.

Our studies are focused on the characterization of the purified NBD portion of HlyB and its H662A[2] derivative, defective in ATP hydrolysis. In this article, we present the enzymatic properties of the wt HlyB-NBD that reveal protein dimerization in the course of the catalytic cycle upon increasing the concentration of enzyme. Analytical gel-filtration provided further evidence for ATP-induced protein dimerization. Detailed analysis of HlyB-NBD in various buffers detected an inverse relationship between activity and stability of the enzyme in solution. Such interdependence demanded the employment of different buffers to monitor activity and gel-filtration behavior of the protein. We also present experimental data consistent with the potential for a sequential mechanism of ATP hydrolysis within the dimeric HlyB-NBD.

MATERIALS AND METHODS

Generation of the Y477W Mutant of HlyB-NBD. To generate the Y477W mutant of HlyB-NBD, plasmid pPSG122 (*17*) was used as template. The mutation was introduced using the ligase chain reaction (LCR) according to the protocol of the manufacturer (Stratagene). Therefore, the primer 5′-tatccggtttcgc**tgg**aagcctgactctcc-3′, where the introduced mutation is highlighted in bold, was employed. After successful amplification, DH5α cells were transformed with a plasmid encoding HlyB-NBD Y477W using standard methods and sequenced to confirm the correct mutation.

Protein Purification. The genes encoding HlyB-NBD, comprising residues 467−707, as well as the mutant proteins H662A (*13*) and Y477W were overexpressed and purified as an N-terminal hexahistidine-tagged fusion protein as described (*18*). Pure 20−50 mg/mL protein in 100 mM CAPS, pH 10.4, and 20% glycerol (storage buffer) was routinely stored on ice for 2−3 weeks, without loss of activity.

ATPase Activity. The ATPase assay was performed as described (*19*) with the following modifications. The dependence of ATP hydrolysis on the nature of buffer and pH was measured at 22 °C in 100 mM of the respective buffering component, plus 20% glycerol, 1 mM ATP, 10 mM $MgCl_2$, and 3.6 μM protein. The protein was first prediluted from storage buffer into a solution of glycerol and ATP (pH of ATP stock solution was adjusted to 7.5−8.0). Reaction buffer was added immediately before the start of the reaction. The assay was initiated by addition of $MgCl_2$.

ATPase activity as a function of enzyme concentration was assayed in 100 mM HEPES, pH 7.0, 20% glycerol, 1 mM ATP, and 10 mM $MgCl_2$ with protein concentrations varying from 72 nM to 3.6 μM. Protein in storage buffer was prediluted in 20% glycerol and 1 mM ATP solution. The reaction was started by the addition of 100 mM HEPES, pH 7.0, 10 mM $MgCl_2$, 1 mM ATP, and 20% glycerol (final concentrations).

To collect data for ATP hydrolysis at varying ATP concentrations, the protein solution was first prediluted into 20% glycerol and aliquoted. After the addition of the corresponding amounts of ATP (0.01−1 mM ATP), the reaction was initiated with 100 mM HEPES, pH 7.0, 10 mM $MgCl_2$, and 20% glycerol (final concentrations). The level of ATPase activity was found to be inversely related to the concentration of $MgCl_2$ in the range of 1−10 mM. For convenience, the highest concentration of 10 mM $MgCl_2$ was used to maintain the same concentration of free Mg^{2+} in all assays.

ATP hydrolysis reactions were run at 22 °C for a time period ranging from 1 min to 2 h, depending on the detected level of ATPase activity. Aliquots (50 μL) were taken at appropriate time points, and the reaction was stopped by addition of 350 μL of 20 mM H_2SO_4. The concentration of inorganic phosphate in the final solution was determined by a colorimetric method (*20*). Absorbance was measured at 620 nm, in 96 well plates, 15 min after the addition of 100 μL dye [0.096% (w/v) malachite green, 1.48% (w/v) ammonium molybdate, and 0.173% (w/v) Tween-20 in 2.36 M sulfuric acid]. All measurements were made under conditions giving a linear rate of product formation (P_i) over time. Calibration of free phosphate concentration was performed with Na_2HPO_4 in the working assay solution. All appropriate controls were taken into account and subtracted, if necessary.

Data were analyzed according to Michaelis−Menten kinetics (eq 1) or the Hill equation (eq 2).

$$v = \frac{v_{max}[S]}{K_M + [S]} \quad (1)$$

$$v = \frac{v_{max}[S]^h}{{K_{0.5}}^h + [S]^h} \quad (2)$$

Here, v denotes reaction velocity, v_{max} the maximal reaction velocity, S the substrate or protein concentration (either ATP or HlyB-NBD), K_M the Michaelis−Menten constant, $K_{0.5}$ the substrate concentration at which 50% of binding sites of enzyme are occupied, and h the Hill coefficient.

Mixing Experiments. Steady-state and time-resolved ATPase activity in the presence of various molar ratios of wt HlyB-NBD and HlyB-NBD H662A were carried out in 100 mM HEPES, pH 7.0, 10 mM $MgCl_2$, 1 mM ATP, and 20% glycerol at a total protein concentration of 1.1 μM. Steady-state experiments were performed for 90 s or 3 min. To access the initial time course of the ATPase activity, reactions with a 1:1 molar ratio of wt and H662A HlyB-NBD (total protein concentration, 1.1 μM) were performed in the above buffer, and liberated inorganic phosphate was determined at

[2] Single and triple letter codes were used for amino acids.

the time points indicated. Using the malachite green assay, we could determine the first time point only after 10 s due to the experimental handling procedure. Data were analyzed according to eq 3 after background correction.

$$v = at + b \tag{3}$$

Here, v denotes the reaction velocity, a the slope of the linear equation, that is, the change of ATPase activity over time, t the time of reaction, and b the y-intercept, for example, the reaction velocity at the infinite reaction time.

Intrinsic Trp-Fluorescence Measurements. Intrinsic Trp-fluorescence measurements of the HlyB-NBD Y477W were performed at 22 ± 1 °C in a Cary Eclipse spectrometer (Varian Instruments) at a protein concentration of 1 μM in 100 mM HEPES, pH 7.0, and 100 mM NaCl. Spectra in the presence of varying concentrations of nucleotides (0−3 mM) were obtained by exciting the sample at 295 nm (slit width 10 nm). Emission spectra were recorded between 305 and 400 nm. To ensure steady-state conditions, spectra were recorded a second time following a 5 min incubation of the protein with the corresponding nucleotides. Under these conditions, less than 10% of the ATP might be hydrolyzed in the presence of Mg^{2+}. Intensities at the peak maximum were determined using the routine provided by the manufacturer. All spectra were background-corrected with spectra recorded for wt HlyB-NBD, which contains a unique Trp (W540), and were adjusted for dilution effects. Background-corrected intensities were analyzed according to eq 4. Here,

$$\frac{F - F_{\min}}{1 - F_{\min}} = 1 - \frac{[S]}{[S] + K_D} \tag{4}$$

F denotes the background-corrected fluorescence, $F_{\min}$ the background-corrected minimal fluorescence at infinite nucleotide concentration, S the nucleotide concentration, and K_D the dissociation constant. Inner filter effects (*21*) of nucleotides were not detected up to nucleotide concentrations of 3 mM and therefore not taken into account in our data analysis.

TNP-Nucleotide Affinity Measurements. Steady-state affinities of TNP-ATP and TNP-ADP to HlyB-NBD were determined at a protein concentration of 1.1 μM at room temperature as described in detail in ref *13*.

Analytical Size Exclusion Chromatography (SEC). A 20−50 mg/mL stock solution of HlyB-NBD (wt or H662A) in storage buffer was diluted to 1−1.9 mg/mL (36−68 μM) into the buffer of interest and incubated in the presence of additives (salts or nucleotides) where necessary. After incubation for 1 h on ice, 50 μL samples were subjected to SEC to assess the stability and/or oligomeric state of the protein. The samples were injected onto a Superdex 75 PC 3.2/30 gel-filtration column (Amersham Pharmacia) equilibrated with the appropriate buffer at 8 °C and were run at 50−75 μL/min. Protein elution was monitored by measuring the absorbance at 280, 290, and 295 nm. Data at 290 and 295 nm were collected to reduce background absorption by the nucleotides, if any. Fractions (50 μL) were collected, and protein content was estimated by SDS−PAGE, if necessary. Elution volumes (in mL) were compared with those of molecular weight standards: BSA (66 kDa), carbonic anhydrase (29 kDa), and hen egg white lysozyme (14.6 kDa). All experimental buffers contained 20% glycerol to protect the protein from precipitation.

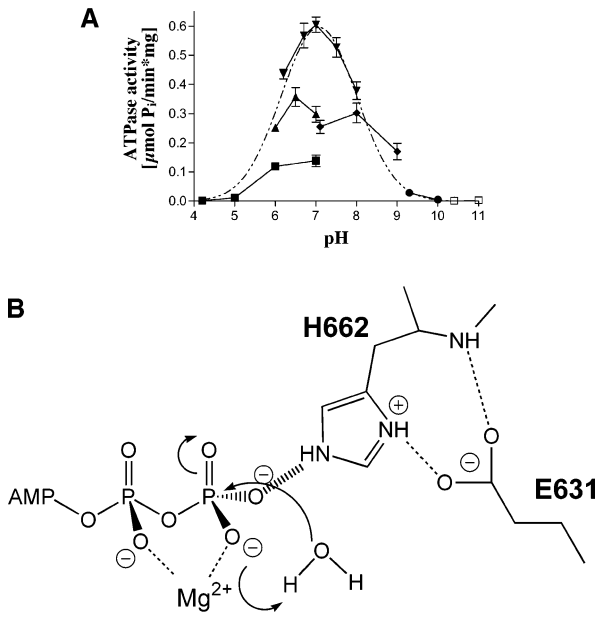

FIGURE 1: Effect of buffer and pH on ATPase activity of the wild-type HlyB−NBD. (A) Buffers used were malonate, pH 4.2−7.0 (closed squares); ADA, pH 6.0−7.0 (closed triangles); HEPES, pH 6.2−8.0 (inverted, closed triangles); Tris, pH 7.1−9.0 (closed diamonds); CHES, pH 9.3−10.0 (closed circles); and CAPS, pH 10.4−11.0 (open squares). ATPase activity at 22 °C was determined from the average of at least three independent experiments with deviations of data points from the mean given as errors. The dashed line shows the fit of the experimental data using a Gaussian function. (B) Structural model explaining the observed pH-dependence. The model was derived from the crystal structure of HlyB-NBD H662A in complex with ATP/Mg^{2+} (*26*). Arrows indicate the molecular steps of the proposed ATP/Mg^{2+}-driven proton abstraction and the nucleophilic attack of the catalytic water.

RESULTS AND DISCUSSION

ATPase Activity of HlyB-NBD in Different Buffers at Various pHs. The majority of studies of isolated ABC-NBDs failed to demonstrate complete functional dimerization of the enzyme in the course of ATPase reaction (*13*, *22*, *23*), thus, hindering a characterization of protein in the fully active state. Although a fully active state of an ABC-NBD might require the presence of the cognate TMD, we suspected that difficulties in obtaining complete functional dimerization of isolated NBDs might reflect non-optimal conditions in which the NBDs were analyzed. Our extensive search for conditions providing HlyB-NBD stability in solution showed that 100 mM CAPS, pH 10.4, and 20% glycerol is the best storage buffer (*18*). Although the protein was functionally inactive in that buffer, the capacity of the enzyme to cleave ATP was easily restored upon dilution of the concentrated protein from storage buffer into various assay buffers. To reveal the most optimal functional buffer, the pH-dependence of HlyB-NBD ATPase activity was investigated using a broad spectrum of pH values and different buffers: malonate (pH 4.2−7.0), ADA (pH 6.0−7.0), HEPES (pH 6.2−8.0), Tris (pH 7.1−9.0), CHES (pH 9.3−10.0), and CAPS (pH 10.4−11.0) (Figure 1A). Hydrolysis of ATP by HlyB-NBD was tested in 100 mM buffer in the presence of 20% glycerol. A high buffer concentration was chosen to maintain a constant

Table 1: Metal Ion Dependent ATPase Activity for Wild-Type HlyB-NBD[a]

cation	Mg^{2+}	Mn^{2+}	Co^{2+}
K_D TNP-ATP/Me^{2+} [μM]	7.23 ± 1.09	6.50 ± 1.07	6.77 ± 0.62
K_D TNP-ADP/Me^{2+} [μM]	2.34 ± 0.31	1.85 ± 0.41	2.62 ± 0.79
$K_{0.5}$ [μM]	332 ± 36	368 ± 28	298 ± 39
k_{cat} [s^{-1}]	0.199 ± 0.004	0.177 ± 0.003	0.056 ± 0.002
$K_{D,app,dimerization}$ [μM]	1.2 ± 0.2	1.3 ± 0.3	1.4 ± 0.3
pK_a[b]	11.4	10.6	8.9
ion radius [Å][b]	0.78	0.91	0.82

[a] Kinetic parameters of the ATP hydrolysis reaction were determined using the Hill equation. [b] Taken from ref 59. Steady-state dissociation constants for the TNP-ATP/Me^{2+}/HlyB-NBD and TNP-ADP/Me^{2+}/HlyB-NBD were determined as described in Materials and Methods. Since we were only interested in relative changes in steady-state affinities in the presence of different metal ions, the fluorophore TNP, covalently attached to the corresponding nucleotides, was used as a reporter. Note that $K_{0.5}$, k_{cat}, and $K_{D,app,dimerization}$ values were determined for ATP.

pH upon generation of free phosphate during the assay. Glycerol was used for protein stabilization in assay solutions.

Normally, a predilution of HlyB-NBD was necessary for assays in different buffers because of the high protein concentration and the presence of CAPS in the storage solution. However, some buffers, such as HEPES, for example, promoted protein aggregation and precipitation, and efforts were taken to limit the time that the protein was exposed to assay buffers. Thus, the HlyB-NBD was usually first prediluted into a buffer-free solution of 20% glycerol and 1 mM ATP. The buffering components were finally added to the assay mixture immediately before starting the reaction with $MgCl_2$ (see below).

Interestingly, the level of ATP hydrolysis was significantly dependent not only upon pH but also upon the buffer itself, with a more than 4-fold variation in v_{max} (Figure 1A). At pH 7.0, the highest ATPase activity for HlyB-NBD was observed in 100 mM HEPES and 20% glycerol (v_{max} = 0.6 μmol ATP/min·mg); the activity was reduced 2-fold in 100 mM ADA and 20% glycerol, or 100 mM Tris and 20% glycerol (v_{max} close to 0.3 μmol ATP/min·mg). The lowest enzyme activity was obtained in 100 mM malonate and 20% glycerol (v_{max} = 0.14 μmol ATP/min·mg). The notion of the inverse relationship between protein stability and level of ATP hydrolysis, for example, was displayed by comparing the properties of CAPS versus HEPES buffer (see also ref *18*) and was supported by further protein analysis (see below).

Despite the specific effect of each buffer on the functional activity of the protein, the pH optimum for ATP hydrolysis stayed close to neutral, regardless of the buffer. ATPase activity sharply declined to an undetectable level below pH 5 and above pH 10. This pH-dependence of the ATPase reaction is reminiscent of other ABC-proteins, such as HisP (*24*) or P-gp (*25*). Using a Gaussian peak distribution, the $v_{max\ 50\%}$ values were determined to be 6.1 and 8.2.

Knowledge of the crystal structure of the HlyB-NBD H662A in complex with ATP/Mg^{2+} (*26*) and the derived "linchpin" model can be used to explain the $v_{max\ 50\%}$ values. This model is summarized schematically in Figure 1B, with H662 playing a key role in catalysis. A pH of 6.2 might correspond to the pK_a values of the side chain of glutamate or aspartate or the γ-phosphate group of ATP, while the pH of 8.2 might reflect the pK_a value of a histidine fixed in a salt bridge (*27*). In the scheme presented in Figure 1B, arrows show the potential pathway of ATP hydrolysis. According to the proposed model, the side chain of His662 forms a salt bridge with the γ-phosphate group of ATP and stabilizes the transition state of the enzyme. ATP, following the principle of substrate-assisted catalysis (*28*), abstracts a proton from the attacking water molecule, which cleaves ATP after nucleophilic attack. Direct interaction of the His with substrate might explain the elevated pK_a value of 8.2 over the intrinsic pK_a of 6.0. Further support for substrate-assisted catalysis (SAC) stems from the fact that modulation of ATPase activity by divalent metal ions (Table 1) is observed. Thus, and in contrast to F_1F_0-ATPase (*29*), turnover numbers for ATPase activity with $Mg^{2+} > Mn^{2+} > Co^{2+}$, as well as the catalytic efficiency ($k_{cat}/K_{0.5}$) (*30*), correlate with the pK_a values of the metal ion−aqua complexes and their strength to act as a Lewis acid but not with their atomic radius. This modulation of activity, which is qualitatively identical to that of P-gp (*31*), implies that a proton abstraction step is influenced by the presence of different metal ions. Moreover, analysis of the dissociation constants of TNP-ATP and TNP-ADP and the dimerization of the HlyB-NBD (see below) revealed that metal ions neither influenced nucleotide affinities nor dimerization of the NBD (Table 1). This is consistent with the idea that the rate-limiting step of the catalytic cycle of the HlyB-NBD is ATP-hydrolysis, that is, a chemical reaction rather than a binding step. In these experiments, for convenience, we employed TNP-fluorophores, which have much higher affinities than unmodified nucleotides. However, since we are only concerned with *relative* differences in affinity due to the presence of different metal ions, TNP-derivatized nucleotides are justifiably used as a valuable reporter. In summary, the data for the pH-dependence of HlyB-NBD activity and the modulation of ATPase activity by divalent metal ions support our recent proposal (*26*) that HlyB-NBD and perhaps other ABC-NBDs utilize SAC during their catalytic cycle.

Positive Cooperativity of ATP Hydrolysis. As shown in Figure 2A, the HlyB-NBD demonstrated a nonlinear dependence of ATPase activity on enzyme concentration over a range of 0.07−1 μM, changing to a constant activity rate at protein concentrations above 2 μM. The relationship between *ATPase activity versus protein concentration* can be described with the Hill equation (eq 2), which is normally used for substrate dependent activity. According to this equation, which describes protein behavior in a statistically relevant manner, the maximal velocity of the reaction, V_{max}, was calculated to be 690 nmol/min·mg at 22 °C, a Hill coefficient h = 1.9 ± 0.1, and kinetic constant $K_{0.5}$ = 1.2 ± 0.2 μM HlyB-NBD. Although these parameters have different meanings compared to the standard definition of the Hill equation, we found them very convenient for the description of the

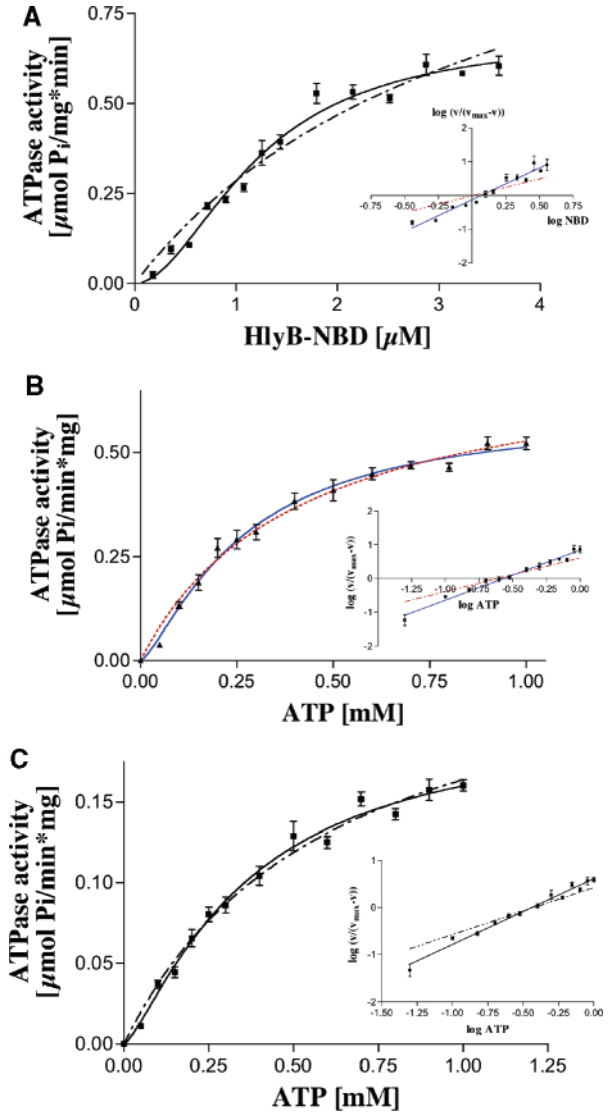

FIGURE 2: (A) ATPase activity of wt-HlyB-NBD at 22 °C. ATPase activity as a function of enzyme concentration in the buffer containing 100 mM HEPES, pH 7.0, 20% glycerol, 10 mM $MgCl_2$, and 1 mM ATP. ATPase activity was determined from the average of at least two independent experiments with the average of the absolute deviations of data points from the mean given as errors. The inset shows a Hill plot of the data. Data were fitted according to Michaelis−Menten eq 1, dashed lines, or Hill eq 2, solid lines. (B) ATPase activity as a function of ATP concentration at a 3.6 μM enzyme concentration in 100 mM HEPES, pH 7.0, 20% glycerol, 10 mM $MgCl_2$, and varying ATP concentrations. ATPase activity was determined from the average of at least two independent experiments with deviations of data points from the mean given as errors. The inset shows the corresponding Hill plot. Data were fitted with a fixed Hill coefficient of 1 (dashed line) or with a variable Hill coefficient (solid line). (C) ATPase activity as a function of ATP concentration at a 1.1 μM enzyme concentration in 100 mM HEPES, pH 7.0, 20% glycerol, 10 mM $MgCl_2$, and varying ATP concentration. ATPase activity was determined from the average of at least two independent experiments with deviations of data points from the mean given as errors. The inset shows the corresponding Hill plot. Data were fitted with a fixed Hill coefficient of 1 (dashed line) or with a variable Hill coefficient (solid line).

functional activity of HlyB-NBD at various protein concentrations. Thus, the Hill coefficient reflects a measure of the degree of cooperativity between monomeric protein subunits, while $K_{0.5}$ indicates the concentration of the monomeric HlyB-NBD required to attain 50% of the saturating reaction activity.

The greater than first-order dependence of ATPase activity on enzyme concentration over the range of 0.07−1 μM of HlyB-NBD (Figure 2A) suggested that the active form of the enzyme is an oligomer, although the equilibrium favors the monomer within this protein range. Formation of the active oligomeric species might therefore be the rate-limiting step at low enzyme concentrations (<1 μM) with the rate of the reaction increasing with protein concentration. A similar dependence of activity on protein concentration was detected for HisP (*22*) and the NBD of the yeast peptide transporter Mdl1p (*23*). In contrast to the aforementioned NBD components, the rate of HlyB-NBD activity became constant at protein concentrations above 2 μM (Figure 2A). In fact, a linear dependence of activity on enzyme concentration was observed only in some special cases of NBDs, such as the independent NBDs, MalK and OpuAA (*32*), or full-length transporters, such as MRP (*33*). MalK, the ABC-component of the *E. coli* maltose transporter (*34*), forms stable homodimers by virtue of its additional 15 kDa C-terminal regulatory domain, even in the absence of nucleotides in solution (*35*). Stable homodimers are very likely organized similarly in OpuAA (*32*), the ABC-NBD of the osmotically regulated ABC-transporter OpuA from *Bacillus subtilis*. Since dimerization is not a rate-limiting step of the ATPase reaction of MalK, OpuAA, and MRP, a linear relationship between ATPase activity and protein concentration is observed. Apparently, the same reason explains the constant activity rate for HlyB-NBD, assuming that an active oligomeric form of HlyB-NBD is also a dimer.

The shape of the curve (Figure 2A) is quite different from a standard hyperbolic function describing protein dimerization. Although several hypotheses can account for the sigmoidal shape of velocity against protein concentration, we favor the existence of spatially separate active sites involved in enzyme dimerization together with a possible interdependence between ATP-binding and dimerization. This notion is further supported by our gel-filtration studies, demonstrating an ATP-induced protein dimerization (see below), and our structural investigations of the HlyB-NBD H662A with ATP/Mg^{2+} (*26*). Accordingly, we set the apparent dimerization constant, $K_{D,app}$, equal to $K_{0.5}$ (1.2 ± 0.2 μM,) as calculated from the experimental data. To the best of our knowledge, this is the first time that a *complete* functional dimerization of the isolated, monomeric ABC-subunits in the absence of regulatory domains or TMDs was observed in the course of the HlyB-NBD ATPase reaction. On the other hand, one has to keep in mind that this number reflects the rate of monomer−monomer interaction for the isolated NBDs of HlyB under the assay conditions. Therefore, one should expect the $K_{D,app}$ to be even lower for the fully assembled HlyB transporter, where strong intermolecular interactions between full-length HlyB, HlyD, TolC, and substrate are observed (*1*, *36*−*38*). Despite this reservation, the protein dimerization constant obtained for the isolated HlyB-NBD under our conditions is about 2 orders of magnitude lower than those calculated for other wild-type NBDs, such as HisP and the Mdl1p-NBD (*22*, *23*), and 1 order of magnitude lower than the experimentally determined K_D value for OpuAA (*32*). In our opinion, the much lower $K_{D,app}$ of 1.2 μM for HlyB-NBD is a result of both the optimized conditions for ATPase assay and the particular

Table 2: Kinetic Parameters of the Wild-Type HlyB-NBD, HlyB-NBD Y477W, and HlyB-NBD H662A[a]

	$K_{0.5}$ [mM]	v_{max} [nmol/mg·min]	k_{cat} [min^{-1}]	h
wt (1.1 μM)	0.36 ± 0.05	202 ± 16	5.6 ± 0.7	1.31 ± 0.13
wt (3.6 μM)	0.26 ± 0.03	600 ± 34	17 ± 1	1.35 ± 0.14
Y477W (1.1 μM)	0.63 ± 0.36	46 ± 8.2	1.3 ± 0.2	1.42 ± 0.34
H662A (up to 0.1 mM)	NM	NM	NM	NM

[a] Parameters were determined according to eq 2. NM, no measurable ATPase activity. Parameters are the average of at least two independent experiments with standard deviations given as errors.

storage buffer for the enzyme, which minimizes protein denaturation.

We also examined the activity of the HlyB-NBD as a function of ATP concentration at two enzyme concentrations, 1.1 and 3.6 μM. The experimental data can be fitted either to the Michaelis−Menten (eq 1) or the Hill (eq 2) equation (Figure 2B,C). At both protein concentrations, the values for the Hill coefficient were indicative of positive cooperativity of ATP hydrolysis and were rather similar, 1.31 ± 0.13 at 1.1 μM and 1.35 ± 0.14 at 3.6 μM (Table 2). The other kinetic parameters significantly depended on the HlyB-NBD concentration (Table 2) and, consequently, on the oligomeric state of the protein (Figure 2A). The apparent affinity of the substrate, Mg/ATP, for HlyB-NBD increased by 100 μM as a result of the monomer−dimer equilibrium (at 1.1 μM), shifting to the predominantly active dimeric state (at 3.6 μM). This change in the oligomeric/functional protein state also affected the ATPase reaction rate, which increased 3-fold attaining a k_{cat} of 17 ± 1 min^{-1} at 3.6 μM NBD.

Thus, the observed activity plots (Figure 2) of the *reaction velocity versus substrate concentration* as well as *versus enzyme concentration* indicate that ATP hydrolysis does not follow Michaelis−Menten kinetics and suggest positive cooperativity between two HlyB-NBD subunits. In conclusion, our results here and previously reported studies of the HlyB-NBD activity (*13*) support the notion of the ATP-induced protein dimerization for isolated ABC-NBDs (*23*, *39*−*41*).

Steady-State Affinity of Nucleotides for the HlyB-NBD Y477W. In all published crystal structures of NBDs of ABC-transporters containing bound nucleotide (*35*, *40*−*46*), the adenine ring moiety interacts with a conserved aromatic amino acid via $\pi-\pi$ stacking. The function of this aromatic amino acid in HlyB is performed by Y477 (*14*), which is located in a loop connecting strand 1 and strand 2 of the ABC-subdomain of the catalytic domain. Replacement of Tyr by Trp in the corresponding position of the protein represents a useful tool to directly monitor nucleotide binding under a wide range of conditions. This procedure avoids the problems associated with the use of fluorescent nucleotides, which normally show increased affinity (*32*) or covalent cross-linking to target proteins. Therefore, we took advantage of this approach for a more detailed characterization of ADP and ATP binding to NBD through engineering of the Y477W mutant. Although the ATPase activity of the purified HlyB-NBD Y477W was about 4-fold lower than that of the wild-type protein (Table 2), the mutant protein displayed quite adequate kinetic characteristics, including positive cooperativity (h = 1.42 ± 0.34) at varying ATP concentrations (Table 2). As expected, titration of HlyB-NBD Y477W with ATP, the nonhydrolyzable ATP analogue AMP-PNP, or ADP (but not AMP), in the presence or absence of the cofactor Mg^{2+}, resulted in nucleotide concentration-dependent quenching of the intrinsic Trp-fluorescence (spectra not shown). After background correction, the data were analyzed according to eq 4 (see Materials and Methods). As summarized in Table 3, the dissociation constants for ADP and ATP are identical within experimental error. This is in clear contrast to data for P-gp, where dissociation constants for ATP and ADP differ by an order of a magnitude (*47*). However, the affinities for both ATP and ADP reported for the isolated N-terminal NBD of MRP-1 (*48*) are in a reasonably close agreement with the results of our studies. In the case of the HlyB-NBD, the presence or absence of the cofactor Mg^{2+} in the nucleotide/HlyB-NBD complexes had no effect on the K_D values (according to our calculations, less than 10% of ATP should be hydrolyzed under the tested conditions). Similarly, Mg^{2+} had little effect on the value of maximal quenching, which depends on the relative orientation of the Trp and the adenine ring (Table 3). This implies that cofactor binding does not induce large conformational changes within the nucleotide-binding site that could influence overall affinity. Nevertheless, one has to be cautious, since the affinity of an NBD toward nucleotides might be modulated by the presence of TMDs. Whether this is true or not in the case of HlyB has to await further functional studies on full-length HlyB.

Table 3: Dissociation Constants of the HlyB-NBD Y477W/ATP, AMPPNP, or ADP Complexes in the Presence or Absence of Mg^{2+} in 100 mM HEPES, pH 7.0, and 100 mM NaCl at 22 °C[a]

	K_D [μM]	B_{max} [au]
ATP	98.3 ± 11.5	0.261 ± 0.005
ATP/Mg^{2+}	87.8 ± 11.2	0.224 ± 0.005
AMPPNP	68.6 ± 5.8	0.271 ± 0.005
AMPPNP/Mg^{2+}	138.0 ± 18.4	0.189 ± 0.006
ADP	89.7 ± 8.8	0.270 ± 0.005
ADP/Mg^{2+}	77.1 ± 13.2	0.244 ± 0.008

[a] Experiments were performed at a protein concentration of 1 μM and nucleotide concentrations ranging from 0 to 3 mM. K_D values were determined as described in Materials and Methods using a "single nucleotide-binding site" model as fit function (eq 4). K_D values are the average of at least three independent experiments with standard deviations given as errors. B_{max} represents the maximal quenching values.

Interestingly, the nearly identical ADP and ATP affinities for the HlyB-NBD also implies that under *in vivo* conditions, where the ratio of ATP to ADP concentration is approximately 10 (*49*), preferential binding of ATP should be ensured, thus, creating directionality in the catalytic cycle of the NBD. In contrast to the absence of a Mg^{2+} effect on the ADP and ATP complexes, the cation changed the affinity of the nonhydrolysable ATP analogue AMP-PNP for HlyB-NBD Y477W by a factor of 2. Whether this is functionally relevant remains questionable, especially since the pK_a value of the γ-phosphate moiety of AMP-PNP is changed upon the introduction of the imino group.

Dimerization, Activity, and Stability of HlyB-NBD and Its H662A Mutant in Various Buffers. Despite the indication of the possible interaction of the HlyB-NBD subunits in the course of ATP hydrolysis, SEC experiments showed that the HlyB-NBD exists predominantly as a monomer in solution (data not shown). HlyB-NBD was typically eluted from the

column at the position corresponding to the 29 kDa protein standard (carbonic anhydrase) in nucleotide-free buffers. Variations in pH, buffers, addition of ATP/ADP up to 1mM, and elevation of protein concentrations up to 70 μM did not induce formation of the dimeric HlyB-NBD species detectable by SEC.

The lack of evidence of oligomerization in SEC experiments for HlyB-NBD is consistent with prior studies of other isolated wild-type ABC-components (*39, 41*), with the only exception of MalK from *E. coli* (*50*) and OpuAA from *B. subtilis* (*32*), both of which contain C-terminal domains assisting protein dimerization. On the other hand, MalK from *Thermococcus litoralis* (*51*) or GlcV (*41*) did not display stable dimer formation despite the fact that both proteins also contain a C-terminal extension. However, the notion of NBD dimerization was supported by studies of many ABC-ATPases and fully assembled ABC-transporters. Thus, the isolated nucleotide-binding subunits of a histidine importer, HisP, a peptide exporter, Mdl1p-NBD, and also HlyB-NBD (see above) showed nonlinear dependence of ATP hydrolysis on enzyme concentration (*22, 23*). Analysis of reconstituted and detergent-solubilized complete transporters for maltose and histidine demonstrated non-Michaelis−Menten kinetics of ATPase activity at various ATP concentrations (*24, 52*). Functional interaction of two MalK monomers was also detected with vanadate-catalyzed photocleavage experiments following ATP hydrolysis (*53*). In contrast to the wild-type NBDs, employment of isolated ABC-subunits with a single amino acid substitution allowed the detection of protein dimerization in the presence of ATP by means of gel-filtration (*23, 39, 41*), fluorescence-binding experiments (*40*), or analytical centrifugation (*39*). The above protein mutations involved either a conservative glutamate or serine within the Walker B or the ABC-signature motif, respectively. Although the above amino acids were postulated to play an important role in the enzymatic catalysis, some ABC-proteins with such substitutions still displayed a significant residual level of ATPase activity (*41, 54*). In the hope of stabilizing a dimeric state of the HlyB-NBD by complete switch-off of ATPase activity, we chose to replace a highly conserved histidine 662 of the H-loop (*12*) with an alanine. Modification of this histidine residue in various ABC-proteins completely abolishes ATPase activity and transport of the allocrite across the membrane by the corresponding transporter, while still preserving protein ATP-binding capability (*55*−*58*). As anticipated, the H662A mutant of HlyB-NBD displayed no ATP hydrolysis under conditions tested for the wild-type protein (Table 2 and Figure 3). Yet, in the nucleotide-free buffers, H662 demonstrated essentially the same behavior as wt HlyB-NBD, being eluted as a single monomeric peak from a gel-filtration column (data not shown).

In SEC experiments, an attempt to employ HEPES buffer, which supported the highest enzyme activity, failed due to the obvious precipitation of the sample over time at the tested protein concentrations. While addition of $MgCl_2$ or NaCl to the HEPES buffer promoted protein stability in the solution, the ATPase activity of the HlyB-NBD in the presence of 100 mM NaCl was only 10% of that in the salt-free buffer (*13*). Thus, an inverse correlation between HlyB-NBD stability and activity was found in HEPES buffer upon salt addition. Since other buffers, although permitting only low or no ATPase activity, maintained protein solubility over a

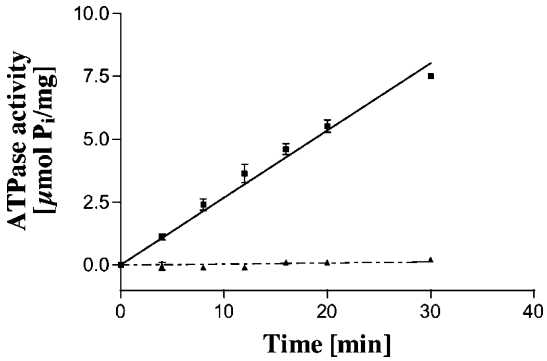

FIGURE 3: ATPase activity of the wild-type HlyB-NBD (squares) and HlyB-NBD H662A (triangles) at 3.6 μM enzyme concentration in 100 mM Tris, pH 8.0, 20% glycerol, 10 mM $MgCl_2$, and 1 mM ATP. Deviations of data points from the mean are given as errors.

sufficiently long period (data not shown), we therefore used malonate (50 mM malonate, pH 5.8, 100 mM sodium acetate, and 20% glycerol) or CAPS storage buffer (100 mM CAPS, pH 10.4, and 20% glycerol) to monitor protein characteristics by gel-filtration. Note that the ATPase activity of the HlyB-NBD is reduced 4−5-fold in malonate compared to the most optimal HEPES buffer, while the protein exists in a reversibly inactive form in CAPS buffer.

The presence of ADP in malonate or CAPS buffers did not alter the mobility of either wt or H662A proteins in gel-filtration experiments (data not shown). However, SEC analysis in the continuous presence of ATP demonstrated a reproducible difference between the wild-type protein and the H662A mutant. Figure 4 shows SEC chromatograms of the proteins in two different buffers: malonate (Figure 4A) and CAPS (Figure 4B). In both buffers, a shift of the monomeric 28 kDa peak of H662A mutant toward a higher molecular mass was observed upon ATP addition. For malonate buffer, at least 1mM ATP was required to observe that shift. The higher the ATP concentration, the more significant was the shift toward the dimer (Figure 4A), approaching an apparent molecular weight of around 50 kDa at 5 mM ATP. The eluted position of the wild-type HlyB-NBD in malonate buffer also showed a small but reproducible shift toward a higher molecular weight, detectable only at 5 mM ATP (Figure 4A). The effect of $MgCl_2$ in addition to ATP or ATP/EDTA was also examined in SEC experiments for both proteins. No detectable differences compared to ATP alone were observed (data not shown). These results are consistent with the notion that ATP induces a rapid equilibrium between dimeric and monomeric forms of HlyB-NBD, while replacement of the conservative histidine with alanine stabilizes the dimeric form of the enzyme in the presence of ATP.

When the wild-type and H662A mutant of the HlyB-NBD were analyzed by SEC in CAPS buffer in the presence of 5 mM ATP (Figure 4B), two peaks were detected. The appearance of the major peak resembled the elution pattern observed in malonate with ATP, while the position of the minor peak or shoulder presumably corresponded to the dimeric protein species of 60 kDa. The presence of two peaks in this elution profile suggested the existence of a slow equilibrium between two species of the enzyme. The shift of the major peak for HlyB-NBD H662A in the ATP-supplemented CAPS could be an indication of either a rapid monomer−dimer equilibrium or ATP binding to the mutant

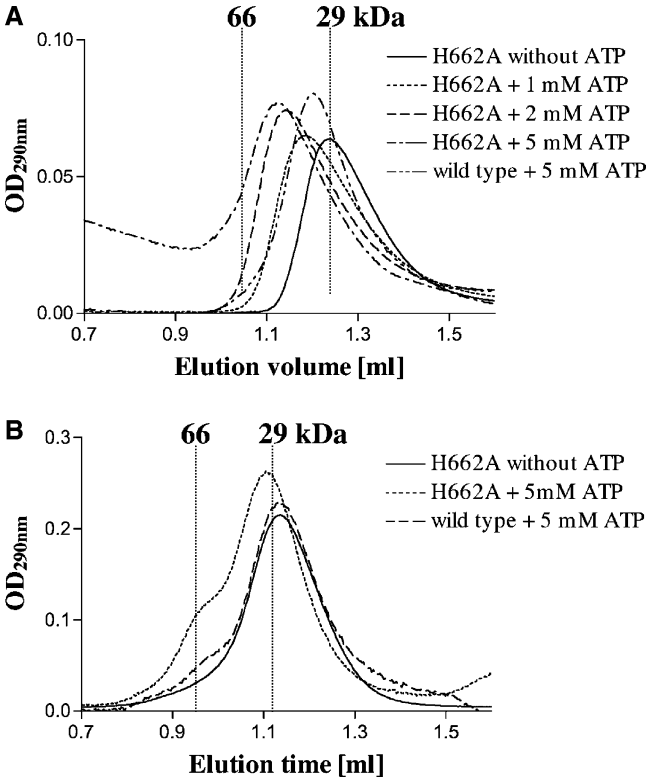

FIGURE 4: Analytical SEC of HlyB-NBD or HlyB-NBD H662A at 50 μM protein concentration. Elution profiles were recorded at 290 nm. (A) Protein mobility in 50 mM malonate, pH 5.8, 100 mM sodium acetate, and 20% glycerol with or without ATP in the running buffer. Note that, for the H662A mutant without ATP, the same protein mobility was observed for the wild-type HlyB-NBD without ATP or for both proteins with ADP (not shown). Note that the protein mobility observed for the wild-type HlyB-NBD without ATP and for both proteins with ADP (not shown) was the same as for the H662A mutant without ATP. (B) Protein mobility in 100 mM CAPS, pH 10.4, and 20% glycerol with or without ATP in the running buffer. Note that the same protein mobility as for the H662A mutant without ATP was observed for the wild-type HlyB-NBD without ATP and for both proteins with ADP.

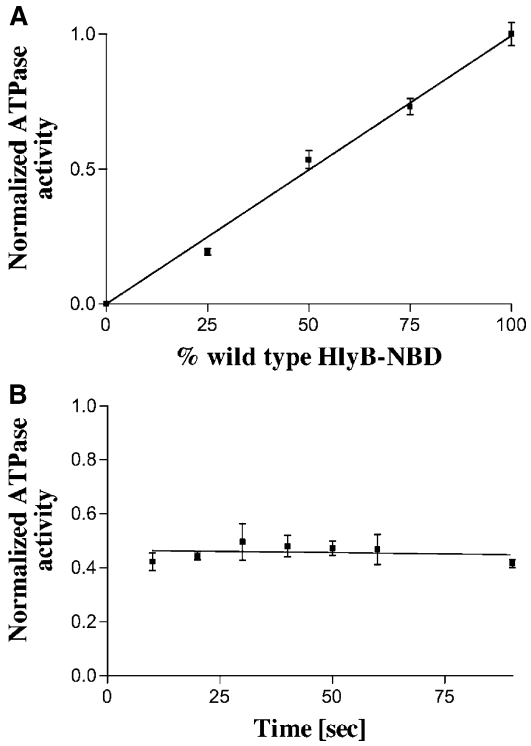

FIGURE 5: ATPase mixing experiments. (A) Steady-state ATPase activity of wt/H662A HlyB-NBD mixture at the indicated molar ratios at 22 °C. Data points represent the average of three independent experiments with the standard deviation given as error bars. Mixtures were prepared as described in Materials and Methods. The v_{max} values were determined after 3 min using the malachite green assay, evaluated according to eq 2, and plotted versus percent (%) of wt HlyB-NBD. The fit was obtained by using a linear regression fit function. (B) Time resolved, initial ATPase activity of a 1:1 molar wild type/H662A HlyB-NBD mixture. Data points were determined as described in Materials and Methods and represent the average of two independent experiments with standard deviations given as errors.

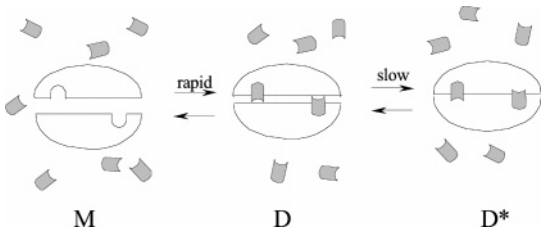

FIGURE 6: Proposed model for dimerization of HlyB-NBD. The model assumes the presence of the two symmetrical ATP-binding sites (*23*, *26*). For further details see text.

protein without inducing dimerization. The latter seems unlikely since binding of ATP causes a major conformation change in the NBD leading to the extensive interaction between the two protein monomers, as we observed in the crystal structure of H662A protein in complex with ATP−Mg (26). Moreover, the presence of ADP, which does not induce dimer formation in crystal structures (*41*, *43*−*45*), did not cause any change in the SEC profile. Thus, we would like to propose the hypothesis that the coexistence of slow and rapid types of equilibria, detected by SEC in CAPS buffer, could be explained by two different dimeric forms of the protein: a form D rapidly equilibrating with the monomeric form (M) and a more stable form D* incapable of the rapid equilibration (Figure 6). The rapid equilibrium seems to be favored by malonate with ATP, the buffer which allows catalysis, while the slow equilibrium and accumulation of D* is supported by CAPS with ATP, the buffer where the protein exists in a latent form lacking activity. It is important to note that changes in protein mobility, including dimer peaks in CAPS, disappeared upon ATP removal from the column buffers (data not shown). This reversible formation of the dimeric species implies that we have observed native conformational/oligomeric changes of the protein state and not a result of protein denaturation/aggregation.

Our studies also demonstrated the significance of the buffer component for protein stability and supported the idea of an inverse relationship between the level of functional activity and stability of HlyB-NBD. Thus, molecules of the buffering component, together with pH, seem to participate actively in the structural rearrangement of HlyB-NBD, altering protein stability and its functional activity.

ATPase Activity of Heterodimers Composed of Wild-Type and H662A HlyB-NBD. To extend further the functional analysis of HlyB-NBD, mixing experiments similar to the ones pioneered for HisP (*55*) were designed. Assuming that the NBD dimer with two ATP-binding sites is a catalytically active species (*23*, *26*, *35*, *39*, *40*), various molar ratios of the ATPase-deficient H662A mutant and the wild-type HlyB-NBD were combined, and steady-state ATPase activity of

the dimers was measured. As shown in Figure 5A, at a constant protein concentration and different molar ratios (3:1, 1:1, and 1:3), a linear relationship of activity versus *amount of the wild-type protein* was observed. Thus, at a 1:1 molar ratio, the steady-state ATPase activity was 50% of the wild-type level. This is consistent with formation of 25% H662A/H662A dimers, 50% H662A/wt, and 25wt % wt/wt dimers, where H662A/H662A homodimers are inactive, wt/wt homodimers are fully active, while H662A/wt heterodimers show half of the wt/wt activity. This result indicates that ATP hydrolysis takes places in one ATP-binding site independent of the other site of the NBD heterodimer. Such a scenario is reminiscent of the model of ATPase activity proposed for Mdl1p-NBD (*23*), which states that the hydrolysis of each ATP molecule in Mdl1p-NBD occurs in a sequential fashion.

The above conclusions are based on the assumption of an unrestricted random association of monomers upon mixing. One can argue that subunits can be associated in a preferential manner, resulting in a favorable formation of the homodimers in the ATP-supplemented solution. In that case, only wt/wt homodimers would be responsible for the detected ATPase activity. However, this scenario seems unlikely in view of a nonlinear dependence of ATPase activity on protein concentration observed in the protein range of 0−1 μM for the wt HlyB-NBD (Figure 2A). Thus, at a 1:1 molar protein ratio of wt and mutant tested at 1.1 μM total protein concentration, the final level of ATP hydrolysis should then be less than 50%, assuming the existence of only homodimers in the solution. The same logic applies to the experiments performed at 25% or 75% of wt proteins in a mixture with H662A mutant. Importantly, the initial ATPase activity of a 1:1 mixture did not change over time. As evident from the data presented in Figure 5B, the initial ATPase activity remained constant during the first 90 s following substrate addition. The first data point was acquired after the first ATPase cycle (k_{cat} is 0.1 ATP s^{-1} under the conditions of the assay). If heterodimers have no ATPase activity, the detected activity would be 25% of that with wt only. After the second ATPase cycle (20 s), an activity of 33.5% would be observed, and so on. However, since no such change in ATPase activity was detectable (Figure 5B), we conclude that the H662A/wt heterodimers must possess 50% of the ATPase activity of the wt/wt homodimer. Thus, we conclude that the linear relationship between activity and increasing the concentration of the mutant NBD (Figure 5A) indicates that both wt/H662A heterodimers and wt/wt homodimers contribute to the detected ATPAse activity.

In HisP, mutations of the corresponding histidine (H211) to arginine or aspartate (*55*) gave different results with respect to ATPase activity of the heterodimers. While the H221R mutation displayed similar results to those described for HlyB-NBD H662A, heterodimers of HisP containing the H221D mutation were ATPase-deficient. On the basis of the recently determined crystal structure of the HlyB-NBD H662 in complex with ATP/Mg^{2+} (*26*), two possible explanations for the latter mutant arise. First, the electrostatic repulsion between the side chain of aspartate and the γ-phosphate of ATP might disrupt the formation of stable heterodimers. However, in our model, H662 of HlyB-NBD forms vital interactions with the D-loop of the trans monomer in the sandwich dimer, which are necessary for monomer−monomer communications. Introduction of an aspartate would severely influence this cross-talk and perhaps prevent ATP-hydrolysis even in a single site. However, further experimental evidence is necessary to determine the precise influence of an aspartate at the position of the conserved histidine.

A Model for ATP-Induced Dimerization and Activity of HlyB-NBD. Functional and gel-filtration studies of both the HlyB-NBD and the H662A mutant, together with the crystal structure of the Mg^{2+}/ATP-bound H662A dimer (*26*), demonstrate that the HlyB-NBD is capable of specifically binding two ATP molecules per dimer and that the dimer serves as the active species for ATP hydrolysis. Binding of ATP but not Mg^{2+}/ATP or ADP promotes dimerization of the isolated NBD subunits. The NBD-dimer can function at a half of its power with one hydrolytically active site even when the other site is defective, although still able to bind ATP. A similar situation is observed for some natural ABC-transporters, where one NBD carries a partially degenerated conserved motif, for example, Pdr5p, RbsA, CFTR, and TAP. In these cases, ATP hydrolysis also occurs independently in one of the active sites of the NBD-dimer.

The combination of activity data and SEC analysis described here suggests that while ATP-induced formation of NBD dimers is a necessary condition for ATP hydrolysis, this may not be sufficient. Thus, two types of ATP-induced dimeric forms of the HlyB-NBD were detected: a hydrolytically active D and reversibly inactive D* state. The former was observed in malonate buffer, while the latter one was the prevailing dimeric state in CAPS buffer.

CONCLUSIONS

Proper storage conditions and adjustment of the preassay procedure for isolated HlyB-NBD significantly optimized the kinetic characteristics of the enzyme by maximally excluding the precipitated and inactive protein from the assay. HlyB-NBD activity and stability were shown to be inversely related. Analysis of protein ATPase activity and SEC experiments provided evidence that a functional form of the HlyB-NBD in catalysis is a dimer. Mutation of the conserved histidine to alanine in the His-loop abolished enzymatic ATPase activity, yet, preserved the ATP-binding capability of the protein. The employment of the H662A mutant of HlyB-NBD allowed us to conclude that one ATP-binding site of the dimer is able to function independently of the hydrolytic capability of the neighboring ATP-binding site. Moreover, we discovered that ATP-promoted dimerization of HlyB-NBD might involve formation of two interconvertible forms: a readily dissociable active dimer and a more stable, reversibly inactive form of the dimer.

ACKNOWLEDGMENT

We thank Carsten Horn, Nils Hanekop, Robert Ernst, Rupert Abele, and Chris van der Does for valuable and stimulating discussions. L.S. thanks R. Tampé for constant encouragement and support. J.Z. thanks Larisa Avramova and Marina Kovina for useful insights.

REFERENCES

1. Holland, I. B., Benabdelhak, H., Young, J., Pimenta, A. L., Schmitt, L., and Blight, M. (2003) Bacterial ABC transporters

involved in protein translocationin, in *ABC Proteins: From Bacteria to Man* (Holland, I. B., Cole, S. P. C., Kuchler, K., and Higgins, C. F., Eds.) pp 209−241, Academic Press (Elsevier Science), London.
2. Koronakis, V., Sharff, A., Koronakis, E., Luisi, B., and Hughes, C. (2000) Crystal structure of the bacterial membrane protein TolC central to multidrug efflux and protein export, *Nature 405*, 914−919.
3. Pimenta, A. L., Young, J., Holland, I. B., and Blight, M. A. (1999) Antibody analysis of the localisation, expression and stability of HlyD, the MFP component of the *E. coli* haemolysin translocator, *Mol. Gen. Genet. 261*, 122−132.
4. Higgins, C. F., Hiles, I. D., Salmond, G. P., Gill, D. R., Downie, J. A., Evans, I. J., Holland, I. B., Gray, L., Buckel, S. D., Bell, A. W., et al. (1986) A family of related ATP-binding subunits coupled to many distinct biological processes in bacteria, *Nature 323*, 448−450.
5. Koronakis, V., and Hughes, C. (1993) Bacterial signal peptide-independent protein export: HlyB-directed secretion of hemolysin, *Semin. Cell Biol. 4*, 7−15.
6. Gottesman, M. M., and Pastan, I. (1993) Biochemistry of multidrug resistance mediated by the multidrug transporter, *Annu. Rev. Biochem. 62*, 385−427.
7. Schmitt, L., and Tampe, R. (2000) Affinity, specificity, diversity: a challenge for the ABC transporter TAP in cellular immunity, *ChemBioChem 1*, 16−35.
8. Ames, G. F., Nikaido, K., Wang, I. X., Liu, P. Q., Liu, C. E., and Hu, C. (2001) Purification and characterization of the membrane-bound complex of an ABC transporter, the histidine permease, *J. Bioenerg. Biomembr. 33*, 79−92.
9. Holland, I. B., and Blight, M. A. (1999) ABC-ATPases, adaptable energy generators fuelling transmembrane movement of a variety of molecules in organisms from bacteria to humans, *J. Mol. Biol. 293*, 381−399.
10. Barroga, C. F., Zhang, H., Wajih, N., Bouyer, J. H., and Hermodson, M. A. (1996) The proteins encoded by the rbs operon of *Escherichia coli*: I. Overproduction, purification, characterization, and functional analysis of RbsA, *Protein Sci. 5*, 1093−1099.
11. Poelarends, G. J., Mazurkiewicz, P., and Konings, W. N. (2002) Multidrug transporters and antibiotic resistance in *Lactococcus lactis*, *Biochim. Biophys. Acta 1555*, 1−7.
12. Schmitt, L., and Tampe, R. (2002) Structure and mechanism of ABC transporters, *Curr. Opin. Struct. Biol. 12*, 754−760.
13. Benabdelhak, H., Schmitt, L., Horn, C., Kiontke, S., Jumel, K., Blight, M. A., and Holland, I. B. (2005) Analysis of the properties of the isolated ABC-ATPase domain of HlyB: activity shows positive co-operativity but dimers appear highly unstable, *Biochem. J. 368*, 1−7.
14. Schmitt, L., Benabdelhak, H., Blight, M. A., Holland, I. B., and Stubbs, M. T. (2003) Crystal structure of the nucleotide-binding domain of the ABC-transporter haemolysin B: identification of a variable region within ABC helical domains, *J. Mol. Biol. 330*, 333−342.
15. Davidson, A. L., and Chen, J. (2004) ATP-binding cassette transporters in bacteria, *Annu. Rev. Biochem. 73*, 241−268.
16. Kerr, I. D. (2002) Structure and association of ATP-binding cassette transporter nucleotide-binding domains, *Biochim. Biophys. Acta 1561*, 47−64.
17. Guzman, L.-M., Belin, D., Carson, M. J., and Beckwith, J. (1995) Tight regulation, modulation, and high-level expression by vectors containing the arabinose *pBAD* promoter, *J. Bacteriol. 177*, 4121−4130.
18. Zaitseva, J., Holland, I. B., and Schmitt, L. (2004) The role of CAPS buffer in expanding the crystallization space of the nucleotide-binding domain of the ABC transporter haemolysin B from *Escherichia coli*, *Acta Crystallogr., Sect. D 60*, 1076−1084.
19. Zaitseva, J., Zhang, H., Binnie, R. A., and Hermodson, M. (1996) The proteins encoded by the rbs operon of *Escherichia coli*: II. Use of chimeric protein constructs to isolate and characterize RbsC, *Protein Sci. 5*, 1100−1107.
20. Baykov, A. A., Evtushenko, O. A., and Avaeva, S. M. (1988) A malachite green procedure for orthophosphate determination and its use in alkaline phosphatase-based enzyme immunoassay, *Anal. Biochem. 171*, 266−270.
21. Faller, L. D. (1989) Competitive binding of ATP and the fluorescent substrate analogue 2′,3′-O-(2,4,6-trinitrophenylcyclohexadienylidine) adenosine 5′-triphosphate to the gastric H+, K+-ATPase: evidence for two classes of nucleotide sites, *Biochemistry 28*, 6771−6778.
22. Nikaido, K., Liu, P. Q., and Ames, G. F. (1997) Purification and characterization of HisP, the ATP-binding subunit of a traffic ATPase (ABC transporter), the histidine permease of *Salmonella typhimurium*. Solubility, dimerization, and ATPase activity, *J. Biol. Chem. 272*, 27745−27752.
23. Janas, E., Hofacker, M., Chen, M., Gompf, S., van der Does, C., and Tampe, R. (2003) The ATP hydrolysis cycle of the nucleotide-binding domain of the mitochondrial ATP-binding cassette transporter Mdl1p, *J. Biol. Chem. 278*, 26862−26869.
24. Liu, C. E., Liu, P. Q., and Ames, G. F. (1997) Characterization of the adenosine triphosphatase activity of the periplasmic histidine permease, a traffic ATPase (ABC transporter), *J. Biol. Chem. 272*, 21883-21891.
25. Urbatsch, I. L., Al-Shawei, M. K., and Senior, A. E. (1994) Characterization of the ATPase activity of purified chinese hamster P-glycoprotein, *Biochemistry 33*, 7069−7076.
26. Zaitseva, J., Jenewein, S., Jumpertz, T., Holland, I. B., and Schmitt, L. (2005) H662 is the linchpin of ATP-hydrolysis in the nucleotide binding doamin of the ABC-transporter HlyB, *EMBO J. 24*, 1901−1910.
27. Yang, J., Yu, M., Jan, Y. N., and Jan, L. Y. (1997) Stabilization of ion selectivity filter by pore loop ion pairs in an inwardly rectifying potassium channel, *Proc. Natl. Acad. Sci. U.S A. 94*, 1568−1572.
28. Dall'Acqua, W., and Carter, P. (2000) Substrate-assisted catalysis: molecular basis and biological significance, *Protein Sci. 9*, 1−9.
29. Papageorgiou, S., Melandri, A. B., and Solaini, G. (1998) Relevance of divalent cations to ATP-driven proton pumping in beef heart mitochondrial F0F1-ATPase, *J. Bioenerg. Biomembr. 30*, 533−541.
30. Fersht, A. (1997) *Enzyme, Structure and Mechanism*, 2nd ed., Freemann, New York.
31. Urbatsch, I. L., Sankaran, B., Weber, J., and Senior, A. E. (1995) P-glycoprotein is stably inhibited by vanadate-induced trapping of nucleotide at a single catalytic site, *J. Biol. Chem. 270*, 19383−19390.
32. Horn, C., Bremer, E., and Schmitt, L. (2003) Nucleotide dependent monomer/dimer equilibrium of OpuAA, the nucleotide-binding protein of the osmotically regulated ABC transporter OpuA from *Bacillus subtilis*, *J. Mol. Biol. 334*, 403−419.
33. Chang, X. B., Hou, Y. X., and Riordan, J. R. (1997) ATPase activity of purified multidrug resistance-associated protein, *J. Biol. Chem. 272*, 30962−30968.
34. Ehrmann, M., Ehrle, R., Hofmann, E., Boos, W., and Schlosser, A. (1998) The abc maltose transporter, *Mol. Microbiol. 29*, 685−694.
35. Chen, J., Lu, G., Lin, J., Davidson, A. L., and Quiocho, F. A. (2003) A tweezers-like motion of the ATP-binding cassette dimer in an ABC transport cycle, *Mol. Cell 12*, 651−661.
36. Balakrishnan, L., Hughes, C., and Koronakis, V. (2001) Substrate-triggered recruitment of the TolC channel-tunnel during type I export of hemolysin by *Escherichia coli*, *J. Mol. Biol. 313*, 501−510.
37. Schlor, S., Schmidt, A., Maier, E., Benz, R., Goebel, W., and Gentschev, I. (1997) In vivo and in vitro studies on interactions between the components of the hemolysin (HlyA) secretion machinery of *Escherichia coli*, *Mol. Gen. Genet. 256*, 306−319.
38. Thanabalu, T., Koronakis, E., Hughes, C., and Koronakis, V. (1998) Substrate-induced assembly of a contiguous channel for protein export from *E.coli*: reversible bridging of an inner-membrane translocase to an outer membrane exit pore, *EMBO J. 17*, 6487−6496.
39. Moody, J. E., Millen, L., Binns, D., Hunt, J. F., and Thomas, P. J. (2002) Cooperative, ATP-dependent association of the nucleotide binding cassettes during the catalytic cycle of ATP-binding cassette transporters, *J. Biol. Chem. 277*, 21111−21114.
40. Smith, P. C., Karpowich, N., Millen, L., Moody, J. E., Rosen, J., Thomas, P. J., and Hunt, J. F. (2002) ATP binding to the motor domain from an ABC transporter drives formation of a nucleotide sandwich dimer, *Mol. Cell 10*, 139−149.
41. Verdon, G., Albers, S. V., van Oosterwijk, N., Dijkstra, B. W., Driessen, A. J., and Thunnissen, A. M. (2003) Formation of the productive ATP-Mg2+-bound dimer of GlcV, an ABC-ATPase from *Sulfolobus solfataricus*, *J. Mol. Biol. 334*, 255−267.
42. Hung, L. W., Wang, I. X., Nikaido, K., Liu, P. Q., Ames, G. F., and Kim, S. H. (1998) Crystal structure of the ATP-binding subunit of an ABC transporter, *Nature 396*, 703−707.

43. Gaudet, R., and Wiley, D. C. (2001) Structure of the ABC ATPase domain of human TAP1, the transporter associated with antigen processing, *EMBO J. 20*, 4964−4972.
44. Karpowich, N., Martsinkevich, O., Millen, L., Yuan, Y. R., Dai, P. L., MacVey, K., Thomas, P. J., and Hunt, J. F. (2001) Crystal structures of the MJ1267 ATP binding cassette reveal an induced-fit effect at the ATPase active site of an ABC transporter, *Structure 9*, 571−586.
45. Yuan, Y. R., Blecker, S., Martsinkevich, O., Millen, L., Thomas, P. J., and Hunt, J. F. (2001) The crystal structure of the MJ0796 ATP-binding cassette. Implications for the structural consequences of ATP hydrolysis in the active site of an ABC transporter, *J. Biol. Chem. 276*, 32313−32321.
46. Verdon, G., Albers, S. V., Dijkstra, B. W., Driessen, A. J., and Thunnissen, A. M. (2003) Crystal structures of the ATPase subunit of the glucose ABC transporter from *Sulfolobus solfataricus*: nucleotide-free and nucleotide-bound conformations, *J. Mol. Biol. 330*, 343−358.
47. Sauna, Z. E., Smith, M. M., Muller, M., Kerr, K. M., and Ambudkar, S. V. (2001) The mechanism of action of multidrug-resistance-linked P-glycoprotein, *J. Bioenerg. Biomembr. 33*, 481−491.
48. Ramaen, O., Masscheleyn, S., Duffieux, F., Pamlard, O., Oberkampf, M., Lallemand, J. Y., Stoven, V., and Jacquet, E. (2003) Biochemical characterization and NMR studies of the nucleotide-binding domain 1 of multidrug-resistance-associated protein 1: evidence for interaction between ATP and Trp653, *Biochem. J. 376*, 749−756.
49. Kashket, E. R. (1982) Stoichiometry of the H+-ATPase of growing and resting, aerobic *Escherichia coli*, *Biochemistry 21*, 5534−5538.
50. Samanta, S., Ayvaz, T., Reyes, M., Shuman, H. A., Chen, J., and Davidson, A. L. (2003) Disulfide cross-linking reveals a site of stable interaction between C-terminal regulatory domains of the two MalK subunits in the maltose transport complex, *J. Biol. Chem. 278*, 35265−35271.
51. Greller, G., Horlacher, R., DiRuggiero, J., and Boos, W. (1999) Molecular and biochemical analysis of MalK, the ATP-hydrolyzing subunit of the trehalose/maltose transport system of the hyperthermophilic archaeon *Thermococcus litoralis*, *J. Biol. Chem. 274*, 20259−20264.
52. Davidson, A. L., Laghaeian, S. S., and Mannering, D. E. (1996) The maltose transport system of *Escherichia coli* displays positive cooperativity in ATP hydrolysis, *J. Biol. Chem. 271*, 4858−4863.
53. Fetsch, E. E., and Davidson, A. L. (2002) Vanadate-catalyzed photocleavage of the signature motif of an ATP-binding cassette (ABC) transporter, *Proc. Natl. Acad. Sci. U.S.A. 99*, 9685−9690.
54. Tombline, G., Bartholomew, L. A., Tyndall, G. A., Gimi, K., Urbatsch, I. L., and Senior, A. E. (2004) Properties of P-glycoprotein with mutations in the "catalytic carboxylate" glutamate residues, *J. Biol. Chem. 279*, 46518−46526.
55. Nikaido, K., and Ames, G. F. (1999) One intact ATP-binding subunit is sufficient to support ATP hydrolysis and translocation in an ABC transporter, the histidine permease, *J. Biol. Chem. 274*, 26727−26735.
56. Shyamala, V., Baichwal, V., Beall, E., and Ames, G. F. (1991) Structure−function analysis of the histidine permease and comparison with cystic fibrosis mutations, *J. Biol. Chem. 266*, 18714−18719.
57. Davidson, A. L., and Sharma, S. (1997) Mutation of a single MalK subunit severely impairs maltose transport activity in *Escherichia coli*, *J. Bacteriol. 179*, 5458−5464.
58. Walter, C., Wilken, S., and Schneider, E. (1992) Characterization of site-directed mutations in conserved domains of MalK, a bacterial member of the ATP-binding cassette (ABC) family [corrected], *FEBS Lett. 303*, 41−44.
59. Basolo, F., and Pearson, R. G. (1967) *Mechanisms of Inorganic Reactions*, John Wiley & Sons, New York.

BI0506122